Nuclear Mathematical and Computational Sciences: A Century in Review, A Century Anew
Gatlinburg, Tennessee, April 6-11, 2003, on CD-ROM, American Nuclear Society, LaGrange Park, IL (2003)

CAPTURING THE EFFECTS OF UNLIKE NEIGHBORS IN SINGLE-ASSEMBLY CALCULATIONS

Kevin T. Clarno and Marvin L. Adams
Department of Nuclear Engineering
Texas A&M University
ktclarno@tamu.edu; mladams@tamu.edu

ABSTRACT

We present our recent progress on improving assembly-level calculations for reactor analysis, including modifications that support a larger *quasi-diffusion* core-level analysis effort. Our main focus is on accurately approximating the effects that neighboring assemblies have on the few-group cross sections, discontinuity factors, and other transport parameters of a given assembly. We also focus on tabulating these effects in an efficient way that allows accurate interpolation by the core-level algorithm. We describe our algorithms and present results from many difficult test problems containing MOX and UO_2 assemblies.

Key Words: reactor analysis, albedo, lattice physics, assembly level, quasi-diffusion

1. INTRODUCTION – THE INTERFACE PROBLEM

One of the main challenges that a reactor analysis methodology faces is obtaining the power distribution and averaged cross sections for an assembly whose neighboring assemblies are significantly different. If the neighbors are identical to the assembly in question, then an excellent approximation to the solution in the assembly can be obtained by solving a two-dimensional single-assembly problem with reflecting boundaries. However, if a neighboring assembly is significantly different, the reflecting boundary condition does not accurately model reality.

Reactor analysts have tried many different approaches to approximating the effects of unlike neighbors on an assembly's averaged cross sections. The most straightforward is to run multi-assembly calculations ("colorsets"), one for each four-assembly permutation that will appear in the core [1,2]. While straightforward in principle, this approach is computationally unwieldy, taxing to the user, and it does not eliminate the need to branch and interpolate on conditions in the neighboring assemblies. Thus, most analysis systems attempt to retain the single-assembly calculation and somehow account for the effects of different neighbors.

In this paper we describe our recent efforts to capture and tabulate the effects of different neighbors on the important parameters of a given assembly. Our effort is part of a larger collaborative project that is developing a new reactor-analysis methodology that uses *quasi*-diffusion equations for core-level analysis [3-5].

Part of the assembly-level methodology described here is to use the following detailed angle- and energy-dependent albedo boundary conditions to represent the effects of an unlike neighbor:

$$\psi_g\left(\underline{r}_s,\underline{\Omega}\right)=\gamma_g\left(\underline{r}_s,\underline{\Omega}\right)\psi_g\left(\underline{r}_s,\underline{\Omega}'\right),\ \underline{\Omega}'\equiv\text{exiting direction that reflects onto }\ \underline{\Omega}. \tag{1}$$

Here ψ is angular flux and γ is our specialized albedo. (A *general* albedo function would relate each incoming $\left(g,\underline{\Omega}\right)$ to *all* outgoing $\left(g',\underline{\Omega}'\right)$.) While albedo boundary conditions have been explored before, our approach is different and offers several advantages, as we describe below. Another part of our system is to invoke superposition to estimate the combined effects of the eight neighboring assemblies that surround a given assembly. In this paper we carefully study the accuracy of the superposition approximation, independent of the accuracy of any albedo boundary conditions.

In Section 2 we explain the core-level quasi-diffusion approach to reactor analysis and the data requirements that this approach places upon the assembly-level code. In Section 3 we describe the results of our multiple analyses. Section 3.1 studies the superposition of the effects of unlike neighboring assemblies, which could significantly reduce the number of required analyses. In Section 3.2 we discuss an albedo approximation that simulates the effects of the colorsets presented in Section 3.1. In Section 3.3 we provide the results from an analysis that combines spatial superposition and our albedo approximation of the boundary condition. Section 4 contains a summary and draws conclusions.

2. REACTOR ANALYSIS METHODOLOGY: PRESENT AND PROPOSED

Today's reactor-analysis methodology is reasonably accurate, despite the use of reflecting boundaries for single-assembly calculations and two-group coarse-mesh diffusion for core-level calculations. Even on the most difficult commercial-reactor problems, the current methodology produces pin-power distributions that err by only a few percent [6,7]. This suggests that radical changes in the methodology are not needed; rather, we should carefully extend the existing methodology to try to capture most of the effects of different neighbors in our assembly calculations and most of the transport effects in our core-level calculations. This should eliminate most of the error in today's calculations.

Today's methodology employs single-assembly calculations to generate "base-case" few-group constants (cross sections, diffusion coefficients, and discontinuity factors), where "base-case" means a given set of parameters such as temperatures, power density, soluble boron or void concentration, etc. The variation of the constants with respect to changes in each parameter is estimated by solving one or more "branch cases" for each parameter. In a branch case on soluble boron concentration, for example, all other parameters are held at their base values, the boron concentration is changed, and the single-assembly calculation is performed. A branch on parameter p generates an estimate of $\mathrm{d}C/\mathrm{d}p$ for each few-group constant C. The parameters that are tabulated are those that are needed to perform the core-level calculation and to reconstruct pin-by-pin powers.

In this paper we describe the single-assembly portion of a larger effort to develop an improved reactor-analysis methodology that is a natural extension of today's methodology. The larger effort replaces the core-level diffusion calculation with a core-level *quasi*-diffusion (QD) calculation.[3-5] QD uses diffusion-like equations that contain transport information in the form of "Eddington" tensors; if the correct tensors are used, then the QD equations yield the correct transport solution. In 2D problems, each component of the tensor is an angular-flux-weighted average of the product of two direction cosines:

$$E_{uv}\left(\vec{r}\right) = \frac{\int_{4\pi} \Omega_u \Omega_v \psi\left(\vec{r},\vec{\Omega}\right) d\Omega}{\int_{4\pi} \psi\left(\vec{r},\vec{\Omega}\right) d\Omega}, \quad u = x \text{ or } y, \quad v = x \text{ or } y. \tag{2}$$

Thus, in addition to the usual few-group cross sections and discontinuity factors, our new single-assembly methodology must generate appropriately averaged Eddington tensors to prepare for later core-level QD calculations.

Our new single-assembly methodology also adds branch cases on parameters that describe the difference between the given assembly and its neighbors. Each branch case will be a single-assembly calculation with albedo boundary conditions that represent the effects of the unlike neighbor, either adjacent or diagonal to the given assembly. The result will be the same type of dC/dp values as are currently generated; there are simply additional p's to consider, p's that describe the unlike neighboring assemblies.

3. RESULTS

The most difficult real-world commercial LWR problems involve LEU assemblies interspersed with MOX assemblies. We have considered several such problems to test our new methodology. We first explore the possibility of superimposing the effects of a single unlike neighbor to represent the effects of multiple unlike neighbors. We then test a two-dimensional albedo that we have developed to approximate the effects of a single unlike neighbor, either adjacent or diagonal to the current assembly. Finally, we combine the albedo boundary condition with the superposition approximation and test the ability of the resulting complete methodology to capture the effects of a set of unlike neighbors.

All of our two-dimensional transport results were obtained with a modified version of TALC, a long-characteristics assembly-level transport code written previously at Texas A&M University [8,9]. Each TALC calculation employed 12 flat-source regions per pin cell, 16 energy groups, 4 polar angles, 8 azimuthal angles per quadrant, and 0.5-mm spacing between rays. Each assembly in our test problems was a uniform lattice of geometrically identical pin cells – there were no water holes. Macroscopic cross sections were calculated from a pin-cell analysis using CASMO-3. The UO_2 fuel pins are all 4.0% enriched. The MOX assembly contains an enrichment grading that ranges from 6% to 10% in total Pu content. The corner pins had 6%, the outer rows had 8%, and the interior had 10%. The circular pins were represented exactly.

3.1. Spatial Superposition of Colorsets

In a "colorset" analysis, an assembly-level calculation is performed for each four-assembly permutation that will appear in the core. Each calculation requires up to ten times the CPU time of a single-assembly calculation and more input from the user. We propose to use spatial superposition of the effects of single unlike neighbors to approximate the effects of multiple unlike neighbors and thus reduce the number of calculations that are needed to cover the entire parameter space of neighboring assemblies.

3.1.1. Superimposing the effects of perturbed neighbors

For each assembly in the core, a "base" calculation of the current assembly is performed using reflecting boundaries to determine the "base" few-group constants (C_{base}). Suppose for the moment that we were willing to perform colorset calculations. Then only a single "colorset" calculation, with three of the given assemblies and one unlike neighbor, would be needed in order to determine the effects of a UO_2 neighbor on an adjacent MOX assembly (red underline in Figure 1) as well as a diagonally opposite one (blue italics in Figure 1). That is, one such colorset calculation would yield the change in few-group constants due to an adjacent neighbor $(dC/dp)_{adjacent}$ and the change due to a diagonal neighbor $(dC/dp)_{diagonal}$.

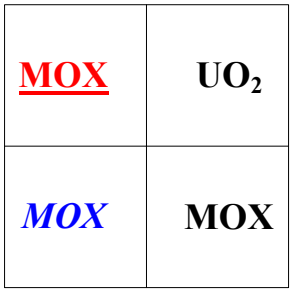

Figure 1. The basic colorset for determining direct effects of a UO_2 on a MOX assembly.

To estimate the effects of multiple perturbed neighbors, we would like to invoke superposition of the effects of single-assembly perturbations. To test the validity of such a superposition we consider three two-dimensional test configurations, as shown in Figure 2. For instance, if a given assembly were surrounded by unlike assemblies (an isolated configuration), then the formula to determine the few-group constants would be:

$$C_{isolated} = C_{base} + \left(dC/dp\right)_{adjacent} + \left(dC/dp\right)_{diagonal} + \left(dC/dp\right)^{T}_{adjacent} . \qquad (3)$$

Because some of the constants (Eddington tensor and boundary current) are spatially and directionally dependant, a transpose-type operation on the adjacent perturbation is required to simulate a neighbor below, as opposed to on the right of, the given assembly.

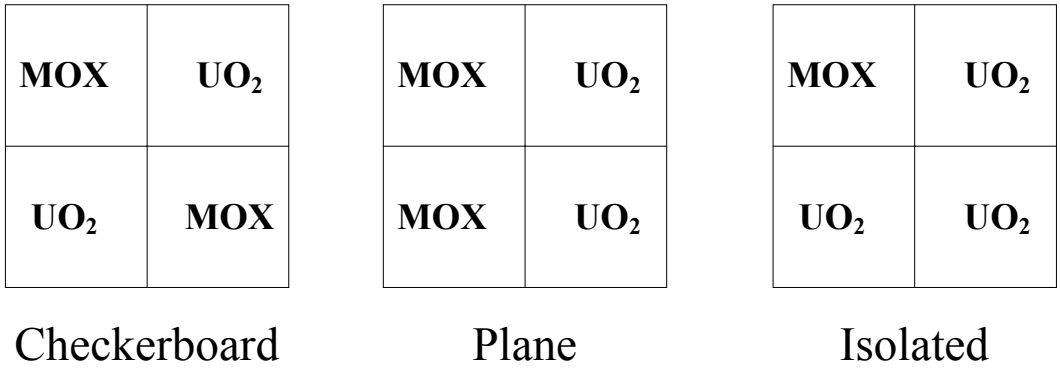

Figure 2. The three 2D test configurations for a MOX assembly.

3.1.2. Results of the superposition tests

We have tested the accuracy of superposition for each of the three test configurations shown in Figure 2, which are tests for computing parameters in the MOX assembly. We have repeated this test for three similar configurations for computing UO_2 parameters. These configurations simply replace each MOX assembly with a UO_2 assembly and vice versa. Thus, we have tested superposition for six different configurations.

For each of the six test configurations, the few-group assembly-averaged cross-sections and Eddington tensors were calculated directly from a four-assembly TALC run to determine the reference value for each of the constants. A "base" case was calculated using a single assembly with reflecting boundaries. Then a fourth four-assembly calculation (basic configuration, shown in Figure 1) was performed to determine the effects on the assembly from an unlike adjacent and unlike diagonal neighbor. Sets of dC/dp's were calculated for these configurations. The base-case parameters and the dC/dp's were then combined as in Eq. 3 to estimate the few-group parameters in the given assembly, and these estimated parameters were compared against the reference values.

The relative cross section errors were similar across all three test configurations for each assembly type. Thus, the results presented for the plane configuration, in Table I, are representative of all three. All of the relative errors of the cross sections are reduced by a factor of 10 or more as compared to the reflecting-boundary case, and the maximum error (which always occurred in the downscattering cross section) in both the UO_2 and the MOX is reduced by a factor of 50. Therefore, the spatial superposition of the effects of a neighbor on cross sections appear to provide an excellent approximation to the exact value, especially when compared against the reflecting-boundary cross sections used in today's methodology. This is very encouraging.

The relative errors of the assembly-averaged transport constants (components of the Eddington tensor) are shown in Table II. The diagonal (E_{xx} and E_{yy}) constants are near 1/3, as expected, and are well approximated by the superposition (maximum error is 0.5%). Superposition errors are

an order of magnitude lower than the reflecting-boundary (base) errors. The off-diagonal E_{xy} value is exactly zero in the base UO_2 (because of no enrichment grading and reflecting boundaries) and very small in the "base" MOX assembly. Therefore, there is no off-diagonal transport data conveyed when simply using the "base" case and the relative error is always ~100%. The superposition does not do a good job of approximating the E_{xy}'s, especially when an unlike "diagonal" assembly is involved. There is a strong effect on E_{xy} with a single unlike assembly diagonal to the given assembly, but this effect is significantly reduced when another unlike assembly is introduced adjacent to the current assembly, as in the plane or isolated configuration. However, in these test problems E_{xy} is very small relative to E_{xx} or E_{yy}, and it is not clear that a large relative error in this component will seriously harm the accuracy of the full-core calculation. This is an issue that we are now investigating.

Table I. Relative errors in the MOX and UO_2 cross sections in plane configurations.

		Relative Error	
	Reference Value	Superposition	Reflecting
MOX Assembly			
2 Group K-inf	1.164	0.00%	-0.12%
Fast Group			
Total	0.506	0.00%	0.24%
Absorption	0.017	0.02%	1.04%
Nu*Fission	0.014	0.00%	0.35%
Fission	0.005	0.00%	0.36%
Inscatter	0.479	0.00%	0.16%
Downscatter	0.011	0.05%	2.19%
Thermal Group			
Total	1.606	0.03%	0.39%
Absorption	0.361	-0.02%	-0.24%
Nu*Fission	0.593	-0.02%	-0.23%
Fission	0.207	-0.02%	-0.21%
Inscatter	1.242	0.04%	0.60%
UO2 Assembly			
2 Group K-inf	1.270	0.02%	-0.26%
Fast Group			
Total	0.508	-0.01%	-0.20%
Absorption	0.010	-0.01%	-0.49%
Nu*Fission	0.008	0.05%	-0.57%
Fission	0.003	0.04%	-0.60%
Inscatter	0.483	-0.01%	-0.13%
Downscatter	0.015	0.03%	-2.09%
Thermal Group			
Total	1.292	0.00%	-0.26%
Absorption	0.106	-0.01%	-0.54%
Nu*Fission	0.169	-0.02%	-0.54%
Fission	0.070	-0.02%	-0.54%
Inscatter	1.184	0.00%	-0.24%

Table II. Relative errors in the MOX and UO_2 Eddington components.

	Reference Value			Spatial Superposition			Reflecting		
	Checker	Plane	Isolated	Checker	Plane	Isolated	Checker	Plane	Isolated
MOX Assembly									
Fast									
E_xx	0.335	0.337	0.336	0.03%	-0.03%	-0.02%	-0.85%	-0.23%	-0.68%
E_xy	2.E-04	-2.E-05	2.E-04	6%	-418%	99%	90%	230%	87%
E_yy	0.335	0.337	0.336	0.03%	-0.01%	-0.02%	-0.85%	-0.25%	-0.68%
Thermal									
E_xx	0.334	0.335	0.336	-0.51%	0.27%	-0.23%	4.85%	5.10%	5.30%
E_xy	2.E-03	-4.E-05	4.E-04	-17%	610%	-180%	104%	-56%	114%
E_yy	0.334	0.321	0.336	-0.51%	0.04%	-0.23%	4.85%	1.00%	5.30%
UO2 Assembly									
Fast									
E_xx	0.341	0.339	0.340	0.01%	-0.02%	-0.02%	0.81%	0.19%	0.62%
E_xy	-4.E-05	6.E-05	1.E-04	-129%	146%	151%	100%	100%	100%
E_yy	0.341	0.339	0.340	0.01%	-0.01%	-0.02%	0.81%	0.24%	0.62%
Thermal									
E_xx	0.361	0.361	0.361	-0.10%	0.06%	-0.05%	-1.25%	-1.27%	-1.28%
E_xy	-9.E-04	-4.E-05	-7.E-04	17%	248%	53%	100%	100%	100%
E_yy	0.361	0.365	0.361	-0.10%	-0.02%	-0.05%	-1.25%	0.01%	-1.28%

3.2. Albedo Boundary Conditions to Simulate the Effects of a Single Perturbed Neighbor

Because of the CPU and user-interface requirements, most reactor analysis code systems today attempt to retain a single-assembly calculation and somehow account for the effects of different neighbors. We propose to work within this framework and to approximate the effects of a neighbor using a "specialized" albedo boundary condition.

3.2.1. One-dimensional albedo approximation

Consider Figure 3's two-dimensional approximation of a real assembly (denoted "L" below) with an unlike neighbor (denoted "R") on one side. If we knew exactly what materials were in region "R", we could solve a two-assembly transport problem to obtain the angular flux, ψ_g, at the interface. At that point we could define:

$$\gamma_g\left(\underline{r}_s,\underline{\Omega}\right)=\psi_g\left(\underline{r}_s,\underline{\Omega}\right)/\psi_g\left(\underline{r}_s,\underline{\Omega}'\right) \quad (4)$$

(If R were a mirror image of L, then γ would equal 1 for each group and angle.) If this energy- and angle-dependent albedo were used as a boundary condition for assembly L, then a single-assembly solution in L would be identical to the two-assembly solution. We wish to avoid solving multi-assembly problems; thus, this definition at first appears to be of little value.

The effect of a "different" neighbor is fairly localized to a good approximation (because thermal neutron mean-free paths are very small compared to the assembly width); thus, much of the interface physics is effectively one-dimensional in space. Further, because γ is a ratio of angular

fluxes, it should be relatively insensitive to symmetric changes in geometric details. We therefore propose to estimate the albedo by solving a 1D problem with two homogeneous regions, as depicted in Figure 4. Each region has the width of a half-assembly, and we employ reflecting boundaries on the outer edges.

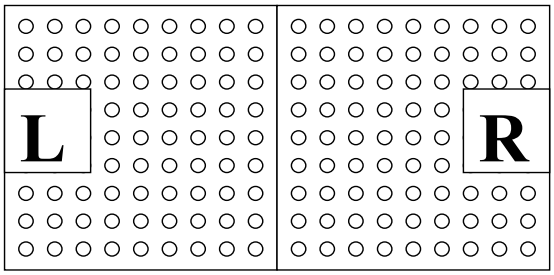

Figure 3. Interface between unlike assemblies

This problem is simple enough that an accurate numerical solution will incur relatively low computational cost. We are using a linear-discontinuous finite-element (LD FE) method in space, multi-group in energy, and discrete-ordinates in angle, with logarithmically spaced spatial zoning at the interface, to quickly calculate the solution, which we then use to estimate the albedo:

$$\gamma_g\left(\underline{r}_s,\underline{\Omega}\right)=\gamma_g\left(\underline{r}_s,\mu,\theta\right)\approx\psi_g^{1\mathrm{DH}}\left(\underline{r}_s,\mu\right)/\psi_g^{1\mathrm{DH}}\left(\underline{r}_s,-\mu\right),\quad \mu=\mathrm{cosine}\left(\underline{\Omega}\bullet\underline{n}\right)<0\ . \tag{5}$$

This approximation provides a significant improvement over the reflecting boundary "base" case, but it still yields appreciable errors near the "corner" interface among four assemblies, as one might expect [10]. Therefore, a two-dimensional modification to the 1D albedo is required to achieve the accuracy we seek.

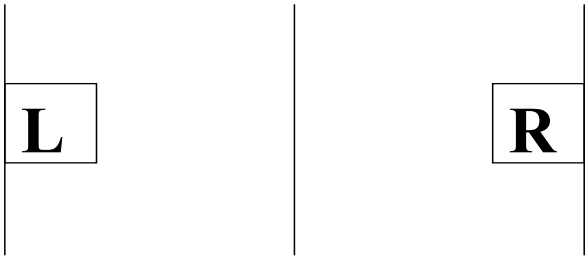

Figure 4. Approximate 1D model of interface between assemblies

3.2.2. Two-dimensional albedo modification

Because the 1D homogeneous albedo produces a very good approximation to the boundary condition away from corner points, a simple modification should be able to account for the 2D effects, which are strongest at corners. Our procedure for obtaining an improved albedo begins by arranging the given assembly (denoted MOX) and the neighbor (denoted UO_2) as shown in Figure 2. Each quarter-assembly is spatially homogenized into pin cells and a simple multi-group, finite-volume diffusion calculation is used to estimate the multi-group, pin-averaged flux shape. This calculation is inexpensive compared to a single-assembly fine-mesh fine-group transport calculation.

The pin cells are then represented as multi-group flat-source regions, with the scattering and fissions sources derived from the finite-volume diffusion solution. Using one simplified long-characteristics sweep, for each azimuthal and polar angle from the assembly-level code's quadrature set, the angular flux at the center of each pin-cell edge on both the L/L and the L/R interfaces are calculated. These angular fluxes are used to calculate a multi-group, pin-cell-edge two-dimensional albedo $\gamma_g^{2D}\left(R_s,\underline{\Omega}\right)$ for each direction used in the assembly-level code.

This 2D albedo is then used to modify the existing 1D homogenous albedo. The albedo of the pin cell nearest the center of the interface between adjacent assemblies is assumed to be exactly the 1D homogenous albedo. The ratio of the 2D albedo on a given pin-cell edge to the 2D albedo at the center-pin edge is then used to modify the 1D albedo:

$$\gamma_g\left(R_s,\underline{\Omega}\right)=\gamma_g^{1DH}\left(\underline{\Omega}\right)*\left[\frac{\gamma_g^{2D}\left(R_s,\underline{\Omega}\right)}{\gamma_g^{2D}\left(R_c,\underline{\Omega}\right)}\right], \tag{6}$$

where R_s is any pin-cell edge along the interface and R_c is the centerline pin cell.

We construct the albedo as in Eq. (6) along both the L/R and L/L interface in the configuration of Figure 2. Different combinations of these albedos and reflecting boundary conditions allow us to model a single adjacent R neighbor or a single diagonal R neighbor; all other R-neighbor configurations can then be built from superposition.

3.2.3. Results of the two-dimensional albedo approximation

For both assemblies in a "basic" colorset configuration, the few-group, assembly-averaged cross-sections and Eddington tensors were calculated to determine the reference value of the "diagonal" and "adjacent" assemblies. A "base" case was calculated using a single assembly with reflecting boundaries. The resulting multi-group assembly-averaged cross sections were used in both the LD FE code, to determine the 1D homogenous albedo, and the diffusion code, to determine an approximate albedo boundary condition for the "diagonal" and "adjacent" configurations. Two single-assembly calculations, using the two-dimensional boundary conditions, were calculated to determine the approximate few-group, assembly-averaged cross-sections and Eddington tensors. Also, a single-assembly calculation using the 1D homogeneous boundary condition was used to provide a "1D" approximation of the constants due to an

adjacent unlike assembly. The 1D and 2D constants were compared, along with the "base" (reflecting-boundary) constants, to the reference values.

The relative cross section errors, shown in Table III, are very small in both "adjacent" and "diagonal" configurations, but the 2D albedo does improve accuracy. In the "adjacent" case, the sign of the error, for nearly all cross sections, changes from the "base" to the "1D approximation", which leads to the expectation that an improved 1D albedo might significantly improve the results. The 2D modification reduces the error of the 1D approximation; the maximum error is less than 1% using the 2D albedo. The most significant improvement occurs in the thermal group in the UO_2 assembly, where the relative error drops to less than 0.02%. In the "diagonal" case, the 2D approximation reduces the error for nearly all cross sections, but with very little change, especially in the fast group, to already small errors.

Table III. 2D approximation of MOX and UO_2 assemblies in diagonal and adjacent configurations.

	Adjacent				Diagonal		
		2D	1D	Reflect		2D	Reflect
	Reference	*Relative Error*			Reference	*Relative Error*	
MOX Assembly							
2 Group K-inf	**1.164**	0.06%	0.07%	-0.07%	**1.164**	-0.03%	-0.04%
Fast Group							
Total	**0.506**	-0.14%	-0.17%	0.12%	**0.506**	0.09%	0.12%
Absorption	**0.017**	-0.42%	-0.55%	0.77%	**0.016**	0.15%	0.26%
Nu*Fission	**0.014**	-0.11%	-0.14%	0.26%	**0.014**	0.07%	0.09%
Fission	**0.005**	-0.12%	-0.15%	0.26%	**0.005**	0.07%	0.10%
Inscatter	**0.479**	-0.12%	-0.13%	0.06%	**0.479**	0.09%	0.11%
Downscatter	**0.011**	-0.89%	-1.25%	1.69%	**0.010**	0.19%	0.47%
Thermal Group							
Total	**1.606**	-0.10%	-0.19%	0.37%	**1.600**	-0.05%	0.00%
Absorption	**0.362**	0.10%	0.29%	-0.12%	**0.362**	0.06%	-0.10%
Nu*Fission	**0.593**	0.09%	0.30%	-0.11%	**0.594**	0.06%	-0.11%
Fission	**0.208**	0.09%	0.29%	-0.09%	**0.207**	0.06%	-0.10%
Inscatter	**1.241**	-0.16%	-0.34%	0.53%	**1.235**	-0.08%	0.03%
UO2 Assembly							
2 Group K-inf	**1.270**	0.03%	0.07%	-0.25%	**1.273**	0.03%	-0.03%
Fast Group							
Total	**0.509**	0.11%	0.14%	-0.10%	**0.509**	-0.08%	-0.09%
Absorption	**0.010**	0.21%	0.26%	-0.30%	**0.010**	-0.14%	-0.18%
Nu*Fission	**0.008**	0.10%	0.16%	-0.47%	**0.008**	-0.04%	-0.15%
Fission	**0.003**	0.13%	0.19%	-0.48%	**0.003**	-0.05%	-0.16%
Inscatter	**0.483**	0.10%	0.12%	-0.04%	**0.483**	-0.08%	-0.08%
Downscatter	**0.015**	0.58%	0.85%	-1.67%	**0.015**	-0.14%	-0.44%
Thermal Group							
Total	**1.292**	-0.02%	0.04%	-0.23%	**1.295**	0.03%	-0.02%
Absorption	**0.106**	-0.04%	0.07%	-0.49%	**0.106**	0.06%	-0.04%
Nu*Fission	**0.170**	-0.04%	0.07%	-0.49%	**0.170**	0.06%	-0.03%
Fission	**0.070**	-0.04%	0.07%	-0.49%	**0.070**	0.06%	-0.03%
Inscatter	**1.184**	-0.02%	0.04%	-0.22%	**1.186**	0.03%	-0.02%

The relative errors in the assembly-averaged Eddington tensors are shown in Table IV. The relative errors in the diagonal (E_{xx} and E_{yy}) components are, in each approximation, not large (under 5%). The 2D albedo reduces the maximum error (thermal-group MOX E_{xx}) by a factor of five to less than 1%. E_{xx} is the transport constant in the direction of the unlike neighbor. The 1D albedo improves the E_{xx} in both assemblies and groups, with a more significant change in the thermal groups. The 2D albedo further reduces the error in the thermal constants, but has the opposite effect in the fast group. A similar trend is seen in the diagonal assembly: a poor modification in the fast groups and an over-modified albedo in the thermal groups (as evidenced by a change in sign of the error).

E_{xy} is approximately zero in the base case; therefore, its error is nearly 100%. Similarly, the 1D approximation of the UO_2 assembly has no effect on E_{xy}, because it is simply a 1D modification to a uniformly enriched assembly. The MOX error is actually increased. The 2D approximation shows improvement in the thermal groups, but decreases the accuracy in the fast groups; the fast UO_2 E_{xy} even has the incorrect sign. We are currently investigating the cause of this poor E_{xy} behavior as well as the significance of such errors when E_{xy} is this small.

The 1D albedo improves accuracy compared to the reflecting-boundary approximation, but is not sufficient to account for the two-dimensional transport effects of the off-diagonal (E_{xy}) component of the Eddington tensor. In addition, the 1D albedo overestimates the effects of the neighbor because it uses an assembly-averaged cross section for an assembly with graded enrichment, which leads to a change in sign of the error. Our 2D modification to the albedo reduces this error in several instances, especially in the thermal group, but in its current form it does not correctly model the off-diagonal Eddington tensor either. We are investigating simple strategies for further improvements.

Table IV. 2D approximation of the Eddington tensor in the adjacent and diagonal configurations.

	Adjacent				Diagonal		
		2D	1D	Reflect		2D	Reflect
	Exact	*Relative Error*			Exact	*Relative Error*	
MOX Assembly							
Fast Group							
E_xx	**0.337**	-0.34%	-0.20%	-0.42%	**0.339**	0.24%	0.22%
E_xy	**1.E-04**	257%	153%	80%	**-2.E-04**	135%	112%
E_yy	**0.337**	-0.19%	-0.15%	-0.46%	**0.339**	0.24%	0.22%
Thermal Group							
E_xx	**0.334**	-0.88%	-1.82%	4.65%	**0.319**	-0.27%	0.22%
E_xy	**1.E-03**	-75%	146%	106%	**-8.E-04**	-103%	92%
E_yy	**0.321**	-0.33%	-0.87%	0.75%	**0.319**	-0.27%	0.22%
UO2 Assembly							
Fast Group							
E_xx	**0.339**	0.19%	0.20%	0.38%	**0.337**	-0.28%	-0.17%
E_xy	**-4.E-05**	565%	100%	100%	**2.E-05**	2665%	100%
E_yy	**0.339**	0.23%	0.13%	0.42%	**0.337**	-0.28%	-0.17%
Thermal Group							
E_xx	**0.361**	-0.01%	0.04%	-1.25%	**0.365**	0.05%	-0.08%
E_xy	**-4.E-04**	-67%	100%	100%	**4.E-04**	-68%	100%
E_yy	**0.366**	-0.03%	0.13%	0.10%	**0.365**	0.05%	-0.08%

In summary, the 2D albedo that we have devised is a computationally efficient way to capture most of the effects that unlike neighbors have on a given assembly. Albedo-based single-assembly calculations produce significantly more accurate few-group cross sections and somewhat more accurate Eddington tensors. We have hypotheses about the causes of the largest remaining errors and ideas for simple ways to improve our albedos and reduce those errors. We will study these in the near future.

3.3. 2D Albedo Boundary Condition Coupled with Spatial Superposition

To fully utilize the single-assembly calculation with albedo boundary conditions and minimize the number of required branches, we must combine spatial superposition with the 2D albedo approximation. In this subsection we test this combination for each of our six test configurations (three for a MOX assembly and three for UO_2). For each configuration we generate a reference solution with a four-assembly TALC calculation. All other solutions in this subsection use TALC only for single-assembly calculations, some with albedo boundary conditions as described above.

A summary of the cross section results is shown in Table V. The highest cross section error is consistently found in the downscatter cross section, so we display this error. In general, there is a reduction in the error as the boundary condition improves from reflecting to 1D albedo to 2D albedo, but the error in the 2D approximation is much greater than the error from the

Table V. Cross-section errors from all tested approximations.

	MOX		UO2	
	Downscatter	2-Group K-inf	Downscatter	2-Group K-inf
Reference values				
Checkerboard	0.0107	1.1632	0.0147	1.2671
Plane	0.0106	1.1635	0.0149	1.2702
Isolated	0.0108	1.1627	0.0146	1.2670
Spatial Superposition				
Checkerboard	-0.05%	0.00%	-0.06%	0.00%
Plane	0.05%	0.00%	0.03%	0.02%
Isolated	0.04%	0.00%	0.01%	0.03%
2D Albedo with Spatial Superposition				
Checkerboard	-1.81%	0.12%	1.12%	0.07%
Plane	-0.66%	0.03%	0.47%	0.07%
Isolated	-1.53%	0.08%	1.06%	0.12%
1D Albedo with Spatial Superposition				
Checkerboard	-2.50%	0.14%	1.68%	0.14%
Plane	-0.74%	0.03%	0.44%	0.06%
Isolated	-1.95%	0.10%	1.30%	0.14%
Reflecting Boundaries				
Checkerboard	3.28%	-0.15%	-3.45%	-0.51%
Plane	2.19%	-0.12%	-2.09%	-0.26%
Isolated	3.80%	-0.19%	-3.85%	-0.51%

superposition of the colorsets (reported in earlier tables). We must investigate further to determine whether further improvements are needed in our albedo boundary conditions; it is possible that they are accurate enough that a different part of our overall methodology is now the limiting factor. As mentioned above, we believe we can devise simple modifications to improve our albedos if this is needed.

The Eddington-tensor results are displayed in Tables VI and VII for UO_2 and MOX, respectively. The E_{xx} and E_{yy} components are very accurate and improve with each improvement in the boundary condition. E_{xx} suffers from inaccuracy as described previously; further investigation will determine whether this is significant. [Note that today's reactor analyses use diffusion theory, which corresponds to E_{xy} =0 and $E_{xx} = E_{yy} = 1/3$.]

Table VI. Eddington-tensor errors from all approximations: UO_2 assembly.

	Fast Group			Thermal Group		
	E_xx	E_xy	E_yy	E_xx	E_xy	E_yy
Reference values						
Checkerboard	0.3407	-4.E-05	0.3407	0.3606	-9.E-04	0.3606
Plane	0.3386	6.E-05	0.3387	0.3606	-4.E-05	0.3652
Isolated	0.3400	1.E-04	0.3400	0.3605	-7.E-04	0.3605
Spatial Superposition						
Checkerboard	0.01%	-129%	0.01%	-0.10%	17%	-0.10%
Plane	-0.02%	146%	-0.01%	0.06%	247%	-0.01%
Isolated	-0.02%	151%	-0.02%	-0.04%	53%	-0.04%
2D Albedo with Spatial Superposition						
Checkerboard	0.43%	1163%	0.43%	-0.14%	-38%	-0.14%
Plane	-0.11%	458%	-0.06%	0.10%	365%	0.00%
Isolated	0.13%	106%	0.13%	-0.04%	23%	-0.04%
1D Albedo with Spatial Superposition						
Checkerboard	0.35%	100%	0.35%	0.07%	100%	0.07%
Plane	0.01%	100%	-0.05%	0.02%	100%	0.03%
Isolated	0.15%	100%	0.15%	0.05%	100%	0.05%
Reflecting Boundaries						
Checkerboard	0.81%	100%	0.81%	-1.25%	100%	-1.25%
Plane	0.19%	100%	0.24%	-1.27%	100%	0.01%
Isolated	0.62%	100%	0.62%	-1.28%	100%	-1.28%

Table VII. Eddington tensor from the superposition of all approximations in the MOX

	Fast Group			Thermal Group		
	E_xx	E_xy	E_yy	E_xx	E_xy	E_yy
Reference values						
Checkerboard	0.3354	2.E-04	0.3354	0.3344	2.E-03	0.3344
Plane	0.3375	-2.E-05	0.3374	0.3353	-4.E-05	0.3214
Isolated	0.3360	2.E-04	0.3360	0.3360	4.E-04	0.3360
Spatial Superposition						
Checkerboard	0.03%	6%	0.03%	-0.51%	-17%	-0.51%
Plane	-0.03%	-418%	-0.01%	0.27%	610%	0.04%
Isolated	-0.02%	99%	-0.02%	-0.23%	-180%	-0.23%
2D Albedo with Spatial Superposition						
Checkerboard	-0.51%	274%	-0.51%	-1.71%	-102%	-1.71%
Plane	-0.13%	-687%	0.04%	-0.87%	281%	-0.57%
Isolated	-0.31%	299%	-0.31%	-1.68%	-314%	-1.68%
1D Albedo with Spatial Superposition						
Checkerboard	-0.32%	166%	-0.32%	-3.15%	149%	-3.15%
Plane	-0.01%	-248%	0.05%	-1.33%	-1019%	-0.61%
Isolated	-0.15%	185%	-0.15%	-2.66%	289%	-2.66%
Reflecting Boundaries						
Checkerboard	-0.85%	90%	-0.85%	4.85%	104%	4.85%
Plane	-0.23%	230%	-0.25%	5.10%	-56%	1.00%
Isolated	-0.68%	87%	-0.68%	5.30%	114%	5.30%

4. CONCLUSIONS

We have developed extensions of present-day reactor-analysis methodology that systematically account for the effects that different neighbors have on a given assembly's few-group constants. One extension is branch cases that generate the effect of unlike neighbors on a given assembly's group constants. Another extension is to use superposition of the effects of neighboring assemblies to reduce the number of branch calculations that are needed to tabulate the effects of all possible neighbor permutations. Finally, we also use energy-, angle-, and position-dependent albedos to simulate the presence of the unlike neighbors in our branch calculations. We have developed and tested a procedure for efficiently estimating these albedos.

We envision two neighbor-assembly branches for each type of neighboring assembly, one for an adjacent configuration and one for diagonal. For each type and configuration we further envision a small number of branches on the neighbor's burnup and one branch with the neighbor containing a control rod. Other branches might be necessary in some applications. For each branch case we estimate an albedo and perform a single-assembly calculation; this fits into the framework of present-day methodology. (The base case corresponds to all identical neighbors – which produces the usual reflecting boundary condition.) The keys to computational efficiency are rapid estimation of albedos, the use of superposition, and keeping the number of branch cases reasonably low. The keys to accuracy are accurate estimation of albedos and careful attention to the limits of the superposition approximation.

We have found that spatial superposition of the effects of adjacent and diagonal neighbors provides an excellent approximation to the effects of multiple neighbors on the assembly cross sections and the diagonal (*xx* and *yy*) Eddington-tensor components. There is a large relative error in the superposition approximation of the very small off-diagonal (*xy*) component, the significance of which has not yet been determined.

We have found that the albedos produced from 1D homogenized calculations do a reasonably good job of capturing the effects of a different neighbor except near assembly corners, although it appears likely that explicit representation of the water gap will add enough accuracy to warrant its complexity. We have devised a 2D homogenized diffusion approximation combined with a fixed-source long-characteristics transport sweep to obtain 2D correction factors for the 1D albedo. This does not cause the off-diagonal tensor component to be accurate, but it does improve the cross sections and diagonal tensor components. Our estimated albedos produce significant improvements over the reflecting condition, but we believe that further significant improvement is possible, and we are actively pursuing such improvement.

We are currently working to couple our assembly-level results with full-core quasi-diffusion calculations to assess the impact of the errors that remain in our cross sections and Eddington tensors. If this assessment shows that further assembly-level improvements will noticeably improve the accuracy of the overall methodology, then we believe we can accomplish these improvements, beginning with simple improvements to our albedo boundary conditions.

In summary, we believe the new methodology described here is promising, and we expect to continue to refine it, couple it to other pieces of a full reactor-analysis system, and test the coupled system. We hope to report on further progress in future communications.

ACKNOWLEDGMENTS

We thank Kord Smith, Dmitriy Anistratov, and Todd Palmer for many helpful discussions. The first author acknowledges the support provided by the Naval Nuclear Propulsion Fellowship Program sponsored by the Naval Reactors Division of the U.S. Department of Energy. This work was also supported through the Nuclear Energy Research Initiative (NERI) Program of the US Department of Energy under grant No. DE-FG03-99SF21922.

REFERENCES

1. D. Knott et al., "CASMO-4 Methodology Manual," STUDSVIK/SOA-95/02, Studsvik of America (1995).
2. K. Smith, "MOX Analysis Methods in SIMULATE-3," *Trans. Am. Nucl. Soc.*, **76**, pp.181 (1997).
3. D. Y. Anistratov, "Homogenization Methodology for the Low-Order Equations of the Quasidiffusion Method," *Int. Conf. on the New Frontiers of Nuclear Technology: Reactor Physics, Safety and High-Performance Computing* (PHYSOR 2002), Seoul, Korea, Oct. 7-10 (2002).
4. R. Nes and T. S. Palmer, "An Advanced Nodal Discretization for the Quasi-Diffusion Low-Order Equations," *Int. Conf. on the New Frontiers of Nuclear Technology: Reactor Physics, Safety and High-Performance Computing* (PHYSOR 2002), Seoul, Korea, Oct. 7-10 (2002).
5. H. Hiruta, D. Y. Anistratov, and M. L. Adams, "Splitting Method For Solving The Coarse-Mesh Discretized Low-Order Quasidiffusion Equations," *this proceedings.*
6. K. Rempe, K. Smith, "Mixed-Oxide and BWR Pin Power Reconstruction in SIMULATE-3," *PHYSOR 90*, Marseille, France, April 1990, Vol. 2, p. VIII-11.
7. S. Palmtag, A. Henry, "Advanced Nodal Methods for MOX Fuel Analysis," Massachusetts Institute of Technology, Nuclear Engineering Department, Ph.D. Thesis, September 1997.
8. M. R. Zika, "Iterative Acceleration for Two-Dimensional Long Characteristics Transport Problems," Texas A&M University, Department of Nuclear Engineering, PhD dissertation (M. L. Adams, advisor) (1997).
9. M. R. Zika and M. L. Adams, "Transport Synthetic Acceleration for Long-Characteristics Assembly-Level Transport Problems," *Nucl. Sci. Eng.*, **134**, pp.135-158 (2000).
10. K. T. Clarno and M. L. Adams, "Improved Boundary Conditions for Assembly-Level Transport Codes," *Int. Conf. on the New Frontiers of Nuclear Technology: Reactor Physics, Safety and High-Performance Computing* (PHYSOR 2002), Seoul, Korea, October 2002, pp. 11A-01.